Life Sciences 232 (2019) 116661

Contents lists available at ScienceDirect

Life Sciences

journal homepage: www.elsevier.com/locate/lifescie

Polyethylenimine-associated cerium oxide nanoparticles: A novel promising gene delivery vector

Leila Hasanzadeh[a], Majid Darroudi[b,*], Navid Ramezanian[c], Parvin Zamani[a], Seyed Hamid Aghaee-Bakhtiari[a,d], Esmail Nourmohammadi[e], Reza Kazemi Oskuee[f,a]

[a] Department of Medical Biotechnology & Nanotechnology, Faculty of Medicine, Mashhad University of Medical Sciences, Mashhad, Iran
[b] Nanotechnology Research Center, Pharmaceutical Technology Institute, Mashhad University of Medical Sciences, Mashhad, Iran
[c] Department of Chemistry, Faculty of Science, Ferdowsi University of Mashhad, Mashhad, Iran
[d] Bioinformatics Research Center, Mashhad University of Medical Sciences, Mashhad, Iran
[e] Neurogenic Inflammation Research Center, Mashhad University of Medical Sciences, Mashhad, Iran
[f] Targeted Drug Delivery Research Center, Pharmaceutical Technology Institute, Mashhad University of Medical Sciences, Mashhad, Iran

ARTICLE INFO

Keywords:
Cerium oxide nanoparticles
Polyethylenimine
Gene delivery
Transfection
Cytotoxicity

ABSTRACT

Aims: The development of highly efficient and low toxic non-viral gene delivery vectors is the most challenging issues for successful application of gene therapy. A particular focus has been on understanding structure-activity relationships for transfection activity and toxicity of polyethylenimine (PEI). During the last decade, the use of cerium oxide nanoparticles (CeO_2-NPs) in biomedicine has attracted much attention due to their pH-dependent antioxidant activity. CeO_2-NPs provide protection normal cells from various forms of reactive oxygen species, but possess innate cytotoxicity and apoptosis to cancer cells. The purpose of this study was to design a new class of gene carriers by low molecular weight PEI (B-PEI 10 kDa) coordination onto CeO_2-NPs.

Main methods: B-PEI 10 kDa was conjugated to CeO_2-NPs by Epichlorohydrin linker. Transfection efficiency, cytotoxic and apoptotic effects of pDNA-PEI-CeO_2 NPs were evaluated on WEHI 164 cancer cells and normal L929 cells lines.

Key findings: PEI-CeO_2 NPs was able to condense the pDNA at carrier/plasmid (C/P) weight ratios of 0.5. The size and zeta potential of pDNA-PEI-CeO_2 NPs were 124 ± 7 nm and 22 ± 2 mV, respectively. The transfection efficacy of synthesized pDNA-PEI-CeO_2 NPs improved and the cytotoxicity was decreased compared to pDNA-PEI. Moreover, pDNA-PEI-CeO_2 NPs induced more apoptosis than unmodified PEI and CeO_2-NPs control groups. pDNA-PEI-CeO_2 NPs displayed more transfection, cytotoxicity, and apoptosis in WEHI 164 cancer cells than normal L929 cells.

Significance: In conclusion, PEI-CeO_2 nanocarriers could act as a potential candidate for gene and drug delivery to cancerous and tumor cells.

1. Introduction

The success of gene therapy is related to development of a delivery system that can efficiently transfer nucleic acids to target cells without causing adverse effects [1]. As a potent group of nonviral gene delivery vectors, cationic polymers spontaneously interact with nucleic acids which protect and compact them to nano-sized nucleic acids carriers, known as polyplexes [2]. Among cationic polymers, polyethylenimine (PEI) is known as a gold standard for polymeric gene delivery [3]. The positively charged amine groups of PEI increase the proton concentration in the acidic pH of endosome, owing to their high buffering capacity, resulting further permeation of water and subsequently DNA release increased by osmotic swelling and rupture of the endosomal membrane which is known as "proton sponge" effect [4,5]. PEI with molecular weight (MW) between 800 and 25,000 Da have been used for gene delivery. High MW PEI is proper for gene delivery, while it has unacceptable cytotoxicity. Low MW PEI is less toxic, but it does not exhibit effective cell transfection and uptake [6,7].

The fact that cells take up nanoparticles can be used to bring nucleic acids into a living cell [8]. Recently, quite a number of oxide

* Corresponding author.
** Corresponding author at: Targeted Drug Delivery Research Center, Pharmaceutical Technology Institute, Mashhad University of Medical Sciences, Mashhad, Iran.
E-mail addresses: darroudim@mums.ac.ir (M. Darroudi), OskueeRK@mums.ac.ir (R. Kazemi Oskuee).

https://doi.org/10.1016/j.lfs.2019.116661
Received 20 April 2019; Received in revised form 13 July 2019; Accepted 15 July 2019
Available online 16 July 2019

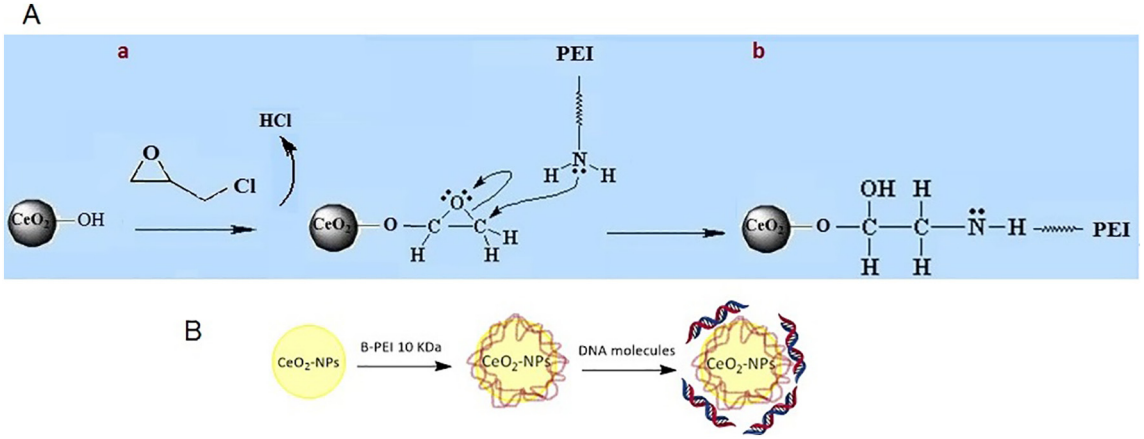

Fig. 1. A) Chemical reaction (nucleophilic substitution) between CeO_2-NPs and B-PEI 10 kDa to form PEI-CeO_2 NPs: a) Epichlorohydrin functionalized CeO_2-NPs; b) B-PEI 10 kDa coated CeO_2-NPs.
B) Schematic showing of pDNA-PEI-CeO_2 NPs.

nanoparticles attract much attention as potential drug and gene delivery carriers due to their versatile physiochemical properties [9]. Cerium is a rare earth element with two oxidation states, Ce (4^+) and Ce (3^+) that can be switched with each other [10,11]. During the last decade, the use of cerium oxide nanoparticles (CeO_2-NPs) in biomedicine has attracted much attention due to their ability in switching oxidation states according to environmental status [12,13], and their specific chemical, physical and biological properties [14–17]. CeO_2-NPs served as natural reactive oxygen species (ROS) scavengers therefore protect normal cells from various forms of ROS generation [18,19]. CeO_2-NPs have pH-dependent antioxidant activity for improved cancer therapeutics, as they provide cytoprotection from free radicals to normal cells, but not to cancer cells, which are typically in an acidic environment, thus they can consider as a therapeutic agent to treatment of cancer via induction of oxidative stress and apoptosis [20,21].

To expand the applications of CeO_2 NPs, scientists are investigating methods to prevent the nanoparticles aggregation in the biological media or within the body [22]. So coating CeO_2-NPs with PEI may be able to prevent them from aggregation. Also there is a possibility to improve gene delivery efficiency and reduce cytotoxicity of PEI by conjugating it to other molecules [23,24]. In this study, PEI 10 kDa was used because of its lower toxicity (in comparison with PEI 25 kDa) [25,26] in order to design a non-viral gene delivery vector consist of B-PEI 10 kDa and CeO_2-NPs with high transfection efficiency and low cytotoxicity.

2. Materials and methods

2.1. Materials

Branched polyethylenimine (B-PEI; MW 10 kDa and 25 kDa) were purchased from Polysciences, USA. Dimethyl sulfoxide (DMSO), 3-(4,5-dimethylthiazol-2-yl)-2,5-diphenyltetrazolium bromide (MTT), trypsin 0.25%, penicillin and streptomycin were purchased from Sigma-Aldrich, Germany. Epichlorohydrin and sodium hydroxide (NaOH) were supplied from Merck, Germany. 4-(2-Hydroxyethyl)-1-piperazineethanesulfonic acid (HEPES), glucose, sodium tetraborate, phosphate buffered saline (PBS), and 2,4,6-trinitrobenzene sulfonic acid (TNBS) were supplied from Sigma-Aldrich, USA. Ethidium bromide was purchased from CinnaGen, Iran. Tris-Borate-EDTA (TBE 5×), DNA green viewer, and loading dye buffer were obtained from Pars tous, Iran. pCMV-EGFP and lysis buffer were purchased from Promega, USA. FITC annexin V apoptosis detection kit with PI was supplied from IQ product, Netherlands. All other used solvents and reagents were chemical grade. Double distilled water (DDW) was used in all steps.

2.2. Cell lines and media

WEHI 164 is a mouse BALB/c fibrosarcoma cell line and L929 is a mouse fibroblast cell line were obtained from the Pasteur Institute, Iran and cultured in Dulbecco's modified Eagle medium (GIBCO, USA) high glucose medium supplemented with penicillin (100 IU/mL), streptomycin (100 μg/mL), and 10% FBS (GIBCO, USA). The cells were maintained in an incubator at 37 °C and 5% CO_2.

2.3. Plasmid preparation

The CMV-EGFP plasmid encoding *enhanced green fluorescent protein* (EGFP) was transformed into *Escherichia coli*-DH5α and extracted by plasmid extraction kit (Qiagen, Germany) according to the manufacturer's instructions. The purity of plasmid DNA (pDNA) was confirmed by agarose gel electrophoresis. Moreover, the pDNA concentration estimated by measuring the absorbance at 260 nm and the ratio of absorbance at 260 nm vs 280 nm using ultraviolet spectrophotometer (Cecil, CE-9500, UK) [27,28].

2.4. Preparation of PEI-CeO_2 NPs

CeO_2-NPs were prepared via green method by applying Chitosan as a stabilizer according to our previously *described* procedure [29]. To form PEI-CeO_2 NPs, CeO_2-NPs were functionalized with Epichlorohydrin through nucleophilic substitution (S_N2) reaction (Fig. 1A) [30]. 25 mg (0.145 mM) of CeO_2 nanopowder was suspended in 5 mL of NaOH (0.1 M) solution under constant stirring for 5 min at room temperature. Then, 2.5 mL of Epichlorohydrin and 0.25 mL of NaOH (2 M) were added to suspension and stirred at room temperature for 8 h. After that, the reaction mixture was centrifuged at 10,000 rpm for 3 min and the supernatants were disposed. The resulting pellet was washed with deionized water (2 or 3 times) followed by centrifugation at 10,000 rpm for 3 min. This was done until the pH of the product (Epichlorohydrin coated CeO_2-NPs) was reached approximately to 7. Finally, the product was dried under vacuum pump system (Vacuubrand, BVC 21, Germany).

Next, 20 mg of B-PEI 10 kDa (0.002 mM) was added to dried mixture (Epichlorohydrin coated CeO_2-NPs) and dissolved in 125 mL of deionized water and stirred for 24 h at room temperature. B-PEI 10 kDa opened the epoxide ring on the Epichlorohydrin molecule to form PEI-CeO_2 NPs (S_N2 reaction) (Fig. 1A). Finally, the reaction mixture was centrifuged at 4000 rpm for 10 min and the supernatants were discarded and resulting pellet was washed with deionized water (3 or 4 times) followed by centrifugation at 4000 rpm for 10 min until the pH

of product (B-PEI 10 kDa coated CeO_2-NPs) was reached to 7 [31].

In order to remove unreacted solvents, the B-PEI 10 kDa coated CeO_2-NPs (PEI-CeO_2 NPs) were dialyzed against deionized water for 24 h (the Spectra/Por dialysis membranes with MWCO of 10 kDa, Spectrum Laboratories, Houston, USA). Finally, PEI-CeO_2 NPs were dried under freeze dryer (Martin Christ, Alpha 2–4 LD plus, Germany).

2.5. Characterization of PEI-CeO_2 NPs

The prepared PEI-CeO_2 NPs were characterized by transmission electron microscopy (TEM) (Carl Zeiss, EM 900, Germany), field emission scanning electron microscope (FE-SEM) (TESCAN, MIRA3, Czech Republic), energy dispersive X-ray spectroscopy (EDX) (Oxford instruments, EDS-6636, UK), and Fourier transform infrared spectroscopy (FTIR) (Perkin Elmer, Spectrum GX, USA).

2.6. Preparation of pDNA-PEI-CeO_2 NPs

For preparation of polyplexes, different concentrations of vectors (C) were separately diluted in 50 μL of HBG buffer (HEPES-buffered glucose, 20 mM HEPES, 5% glucose, pH 7.4) and mixed with 50 μL of pDNA (P) diluted in the HBG buffer (2 μg/50 μL). According to PEI-CeO_2/pDNA weight ratios (C/P), PEI-CeO_2 NPs were added to pDNA (pCMV-EGFP) and after gentle mixing, solution was incubated at room temperature for 20 min to form the polyplexes.

2.7. Determining size and zeta potential of polyplexes

The particle size and zeta potential of the pDNA-PEI-CeO_2 NPs were measured by dynamic light scattering (DLS) using a Zetasizer (Malvern, Nano ZS, UK) at C/P 1. For this purpose, 5 μL of 1 mg/mL of PEI-CeO_2 NPs were diluted in 120 μL HBG buffer and added to an equal volume of the same buffer containing pDNA (5 μg pDNA in 125 μL HBG). After 20 min incubation, polyplexes size and zeta potential were measured. All measurements were performed triplicate and the results reported as mean ± SD.

2.8. Ethidium bromide exclusion assay (DNA condensation capacity)

The DNA condensation capacity of PEI-CeO_2 NPs was performed using ethidium bromide (EtBr) exclusion assay according to the method described by Askarian et al. [32]. EtBr as a DNA-intercalating dye, when interacted with double-stranded pDNA, emits fluorescence. The condensation of pDNA by PEI-CeO_2 NPs was assessment by decrease in fluorescence intensity of EtBr. The fluorescence intensity of HBG buffer (pH 7.4) containing the 0.4 μg/mL EtBr and 5 μL of 1 mg/mL of pDNA was determined using a spectrofluorometer (Jasco, FP-6200, Japan). The excitation and emission wavelengths were 510 and 590 nm, respectively. At first, the fluorescence intensity of EtBr/DNA solution was set to 100% and then the fluorescence intensity change was measured by adding stepwise 2.5 μL of PEI-CeO_2 NPs (1 mg/mL) to the EtBr/DNA solution. All measurements were performed in triplicate and the results reported as mean with SD. Graph was constructed by plotting the relative fluorescence intensity (%) against the C/P ratios (w/w).

2.9. TNBS assay (amount of B-PEI 10 kDa amines grafted to CeO_2-NPs)

The amount of primary amines of PEI-CeO_2 NPs was determined by TNBS assay according to the method described by Snyder et al. [33]. The values of grafting degrees were determined using the differences between the amounts of primary amines groups on unmodified B-PEI 10 kDa compared to PEI-CeO_2 NPs.

2.10. Gel retardation assay (DNA condensation ability of the PEI-CeO_2 NPs)

To evaluate the condensation ability of PEI-CeO_2 NPs with pDNA in different C/P ratios, gel retardation assay was used. The tightly condensed DNA could not migrate through the agarose gel. After 20 min incubation of PEI-CeO_2 NPs with pDNA (0.5 μg per well) in different C/P ratios, 10 μL of the polyplexes was mixed with 1 μL of green viewer dye and loaded into individual wells on agarose gel 1% at 100 mV in the TBE 1× buffer. Naked pDNA was utilized as a control. After 20 min, DNA bands were visualized under gel documentation (gel imager) (Syngene, U: Genius, India).

2.11. Transfection efficiency and cytotoxicity assay

Transfection efficiency and cell viability assay of pDNA-PEI-CeO_2 NPs were investigated by WEHI 164 cancer cells and L929 normal cells using CMV-EGFP plasmid as described previously [32,34]. Cells at a density of 1×10^4 cells/well were seeded in 96-well plates and incubated in 37 °C and 5% CO_2 for 24 h. Polyplexes were prepared at different C/P ratios (0.4 μg plasmid/well) in the range 2 to 6 (w/w) and then were added to each well containing fresh DMEM medium (100 μL) without FBS and incubated for 4 h. Identical concentration of B-PEI 10 kDa was use as control. After 4 h incubation, the medium was removed and replaced with fresh DMEM medium supplemented by FBS and cells were incubated for an additional 24 h.

Then, for transfection experiment, after 24 h incubation, the medium was removed and lysis buffer was added to each well. The fluorescence intensity of EGFP was measured using a fluorescent plate reader (Perkin-Elmer, VICTOR X5, USA) at excitation 485 nm and emission 535 nm. Also in order to visualize the transfection results, fluorescence microscope (Nikon, Eclipse E200, Japan) was used to capture images of expressed EGFP protein within the cells.

For cytotoxicity experiment, after 24 h incubation, the incubation solutions were aspirated and 10 μL of MTT (5 mg/mL dissolved in PBS) was added to each of the wells and incubated for 4 h. After 4 h, the medium was discarded and 100 μL of DMSO was added to each well to dissolve the formazan crystals formed by live cells. The color intensity of the resulting solution was recorded at 540 nm (630 nm as reference) by a 96-well plate reader (BioTek, Epoch, USA). The relative cell viability was expressed as the percentage of living cells compared to untreated control cells with 100% viability.

Also identical concentration of PEI 25 kDa as gold standard among non-viral vectors was used as control at C/P 0.8. At the C/P ratio of 0.8, the best transfection efficiency with lowest cytotoxicity has reported [35,36]. Transfection and cytotoxicity experiments were carried out in five replications and the results reported as mean with SD.

2.12. Apoptosis assay

1×10^5 cell per well of WEHI 164 and L929 cells were seeded in 24-well plates and incubated for 24 h. Polyplexes (pDNA/vector) containing 4 μg plasmid/well were prepared at C/P 4 and then were added to each well containing fresh DMEM medium (1000 μL) without FBS and incubated for 4 h. After 4 h incubation, the medium was removed and replaced with fresh DMEM medium supplemented by FBS and cells were incubated for an additional 24 h. Identical concentrations of B-PEI 10 kDa and CeO_2-NPs were used as control groups. For preparation of pDNA-CeO_2 NPs, identical concentration (C/P 4) of CeO_2-NPs was diluted in HBG buffer and was added to pDNA diluted in the HBG buffer and after gentle mixing, solution was incubated at room temperature for 20 min.

Thereafter, the apoptosis assay was performed by Annexin V/PI detection kit according to manufacture instructions as mentioned elsewhere [37] and analyzed by flow cytometer (Becton Dickinson, FACSLyric, USA). The results provided as dot plots. The dot plots were

divided into four quadrants using FlowJo software. In FACS plots, necrotic cells represented in the upper left quadrant (Q1) (Annexin V^-, PI^+), Late apoptotic and dead cells indicated in the upper right quadrant (Q2) (Annexin V^+, PI^+), Early apoptotic cells displayed in the lower right quadrant (Q3) (Annexin V^+, PI^-), and live cells shown in the lower left quadrant (Q4) (Annexin V^-, PI^-) [38,39]. The percentage of the Q1 + Q2 + Q3 reported as mean of the apoptotic and necrotic cells. Apoptosis experiment was performed in triplicate and the results expressed as mean with SD.

2.13. Statistical analysis

Data were analyzed using one-way analysis of variance (ANOVA) and two-way analysis of variance (ANOVA). Tukey's post-test and Sidak's multiple comparisons test were performed to assess the significance of the differences among different groups. All statistical analyses were performed using Graph Pad Prism 6 Software. The $P \leq 0.05$ was considered as statistically significant. *Means *P*. value < 0.05, ** means *P*. value < 0.01, *** means *P*. value < 0.001, and **** means *P*. value < 0.0001.

3. Results

3.1. Preparation and characterization of PEI-CeO_2 NPs

B-PEI 10 kDa was successfully conjugated to CeO_2-NPs. The attachment of PEI to CeO_2-NPs was confirmed by TEM, FE-SEM, EDX (EDS), and FTIR methods. The synthesized PEI-CeO_2 NPs (Fig. 2) were well dispersed in distilled water and did not precipitate even after 24 h.

3.1.1. TEM

PEI-CeO_2 NPs were dried under freeze dryer and then their morphology and structure were confirmed by TEM. Fig. 3A displays the TEM images of synthesized PEI-CeO_2 NPs with different magnifications. TEM observation was revealed that this material consists of a scaffold of PEI that embraced CeO_2-NPs. The dark color in the center is attributed to CeO_2-NPs and the light colored around the center can be attributed to PEI.

3.1.2. FE-SEM

The topography of PEI-CeO_2 NPs was investigated by FE-SEM (Fig. 3B). FE-SEM images revealed porous structure with uniform size and shape. Also comparison between FE-SEM images of CeO_2-NPs and PEI-CeO_2 NPs showed that a layer of PEI polymer was covered on the surface of CeO_2-NPs after conjugation (Fig. 3C).

As shown in Fig. 3C, in the similar magnification (200 KX), view field of CeO_2-NPs image is 0.692 μm and increases to 0.924 μm in PEI-CeO_2 NPs image. This is consistent with FTIR results (Fig. 5), in which wavenumbers 3281 and 3358 cm^{-1} in PEI spectrum increase to 3391 cm^{-1} in PEI-CeO_2 NPs spectrum. The main reason behind these increases is covering of CeO_2-NPs by PEI.

3.1.3. EDX

Chemical characterization and elemental analysis of a PEI-CeO_2 NPs were studied by EDX. The EDX spectrum (Fig. 4) showed characteristic peaks of cerium (Ce), oxygen (O), and nitrogen (N). No peak was observed for carbon (C), because EDX analysis has low sensitivity for elements with low atomic number. Moreover, no other peaks were detected that could be related to any phase impurity.

Based on elemental composition via EDX analysis, the amount of B-PEI 10 kDa and CeO_2-NPs in PEI-CeO_2 NPs were determined to be 65% and 35% respectively. Moreover, elemental analysis of PEI-CeO_2 NPs was confirmed via gravimetric analysis. In this method, 18.8 mg of PEI-CeO_2 NPs were heated in an electric muffle furnace (Finetech, SEF-101P, South Korea) at the 600 °C (according to thermogravimetric analysis (TGA/DTA) of PEI) at the heating rate of 4 °C/min for 2 h. At this temperature, PEI was burnt (12.3 mg) and resulting product (6.5 mg) was pure CeO_2-NPs.

Fig. 2. The lab photograph of synthesized B-PEI 10 kDa coated CeO_2-NPs (PEI-CeO_2 NPs).

3.1.4. FTIR

The cooperation between B-PEI 10 kDa and CeO_2-NPs was analyzed by FTIR in the wavenumber range of 400–4000 cm^{-1}. As shown in Fig. 5 in B-PEI 10 kDa spectrum, two main bands at 3281 and 3358 cm^{-1} are assigned to NH_2 stretching; in PEI-CeO_2 NPs spectrum, due to nucleophilic attack of PEI to CeO_2-NPs, these two bands converted to new one main band at 3391 cm^{-1} which represented NH vibration. As shown in Fig. 1A, NH_2 groups of PEI attacked to the epoxide ring on the Epichlorohydrin functionalized CeO_2-NPs, and then converted to NH group in PEI-CeO_2 NPs. Also this S_N2 reaction has led to a change in the wavenumbers and a decrease in the area under the curve

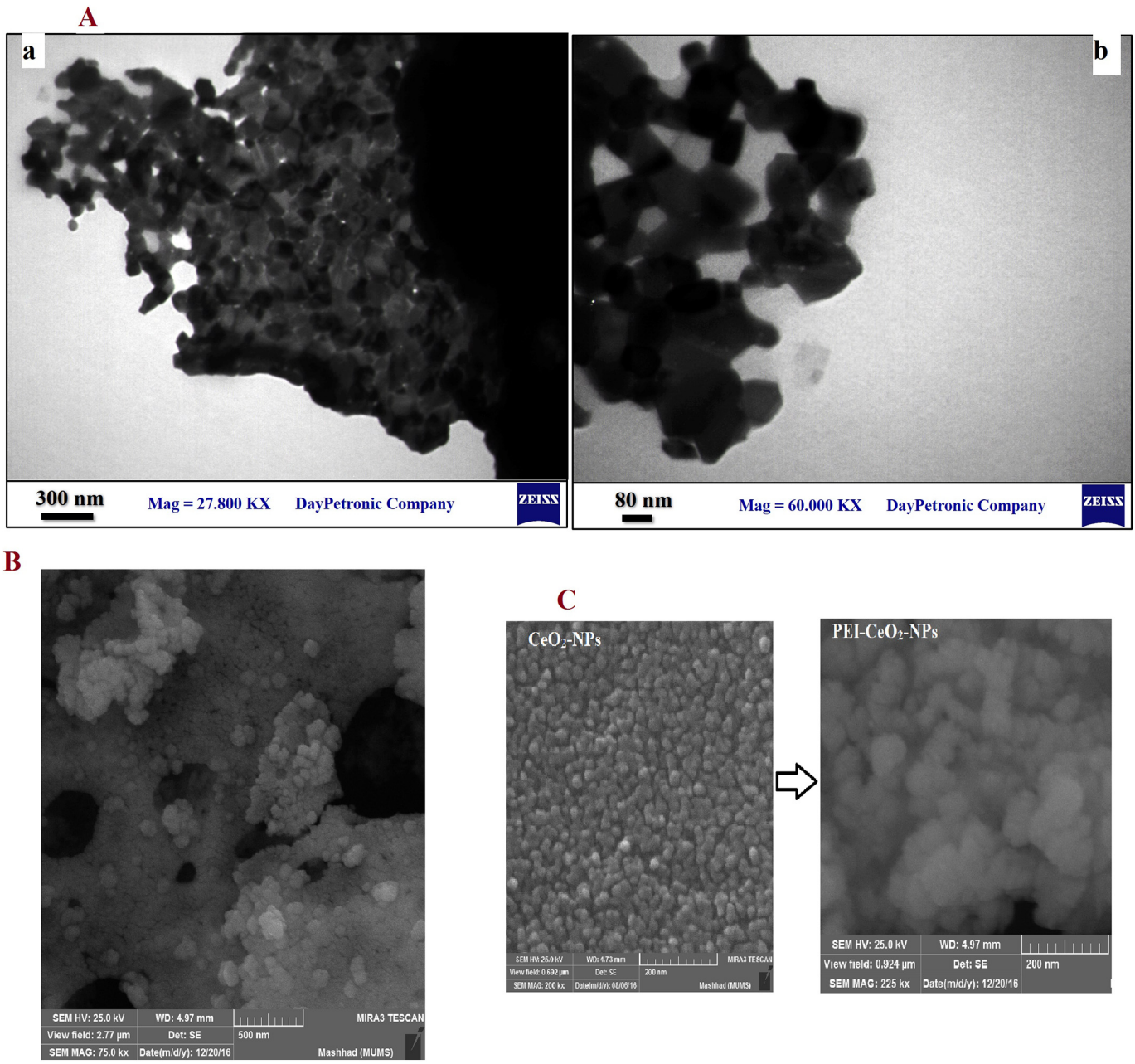

Fig. 3. Microscopic images of PEI-CeO_2 NPs.
A) TEM images of synthesized PEI-CeO_2 NPs with different magnifications: a) 27.800, b) 60.000k×.
B) FE-SEM image of synthesized PEI-CeO_2 NPs, magnification 75.0k×.
C) Comparison between FE-SEM images of CeO_2-NPs and PEI-CeO_2 NPs.

in PEI-CeO_2 NPs spectrum.

3.2. Determination of size and zeta potential of the pDNA-PEI-CeO_2 NPs

The size (*Z*-average) and zeta potential (surface charge) of pDNA-PEI-CeO_2 NPs and pDNA-PEI 10 kDa were summarized in Table 1 (polydispersity index (PDI): 0.405).

3.3. Evaluation of DNA condensation with PEI-CeO_2 NPs

As shown in Fig. 6A, PEI-CeO_2 NPs efficiently condensed pDNA at C/P ratio of 0.5 and reduced the fluorescence intensity of EtBr solution by > 70%.

3.4. Gel retardation assay

As shown in Fig. 6B, when the C/P ratios of pDNA-PEI-CeO_2 NPs were 2, 4 and 6, the pDNA band disappeared on the agarose gel. This result showed that PEI-CeO_2 NPs as nanocarriers could condense pDNA efficiently, and pDNA could be completely loaded to PEI-CeO_2 NPs above the C/P ratio of 1.

3.5. TNBS assay

CeO_2-NPs grafting resulted in decreasing the primary amine content of B-PEI 10 kDa. The standard curve of B-PEI 10 kDa was depicted with different concentrations to achieve its standard equation (data not shown). With the calculations based on the absorbance of the PEI-CeO_2

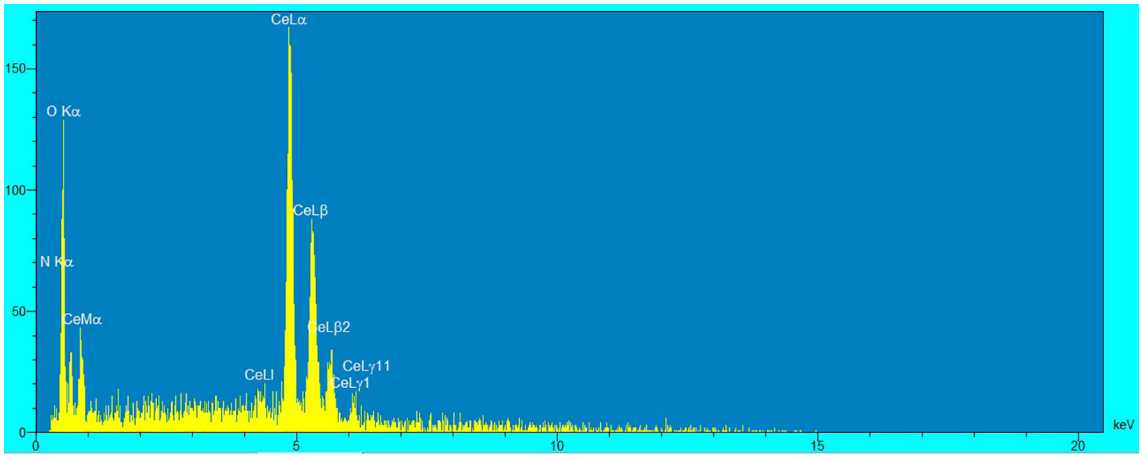

Fig. 4. EDX spectrum of synthesized PEI-CeO_2 NPs.

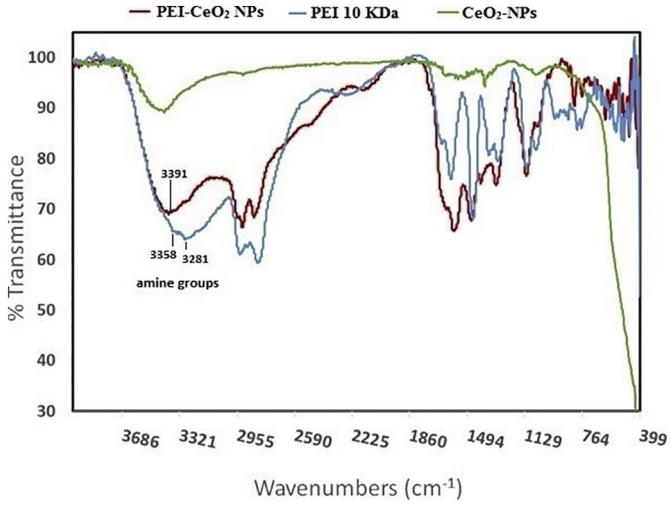

Fig. 5. FTIR spectrum of PEI-CeO_2 NPs, PEI 10 kDa, and CeO_2-NPs.

Table 1
Mean size and zeta potential of pDNA/carrier complexes at C/P ratio of 1.

Nanoparticles	Size (nm) ± SD	Zeta potential (mV) ± SD
pDNA-PEI 10	87 ± 2	24 ± 3
pDNA-PEI-CeO_2	124 ± 7	22 ± 2

NPs (8 μg/100 μL in borate buffer) and the standard equation, the real CeO_2-NPs substitution was determined. The TNBS assay demonstrated that the degree of substitution of CeO_2-NPs on B-PEI 10 kDa was 40.6% from initial percentage of polymer.

3.6. Transfection efficiency

To determine the transfection efficacy of pDNA-PEI-CeO_2 NPs, the fluorescence *value* of EGFP expression was measured in WEHI 164 and L929 cells. In L929 cells (Fig. 7A), the transfection efficacy of prepared pDNA-PEI-CeO_2 NPs improved compared to pDNA-PEI 10 kDa at the C/P 2, 4, and 6. In WEHI 164 cells (Fig. 7B), the transfection efficacy of prepared pDNA-PEI-CeO_2 NPs improved compared to pDNA-PEI 10 kDa at the C/P 4 and 6. Transfection efficacy was increased by increasing C/P ratios in both L929 and WEHI 164 cells ($P < 0.05$).

There was a significant difference in transfection efficacy of pDNA-PEI-CeO_2 NPs between normal cells (L929) and cancer cells (WEHI 164), so that transfection efficacy in WEHI 164 cells was higher than L929 cells at the C/P 2, 4, and 6 (Fig. 7C).

Also the green fluorescence intensities of cells were qualified using fluorescence microscopy. Expression of pDNA was detected as fluorescent images (Fig. 7D).

Moreover, in both L929 and WEHI 164 cells, the transfection efficiency in pDNA-PEI-CeO_2 NPs at the C/P 6 was almost the same as pDNA-PEI 25 kDa (C/P 0.8).

3.7. Cytotoxicity assay

The cytotoxicity of pDNA-PEI-CeO_2 NPs was evaluated by the MTT assay. The cell viability decreased by increasing C/P ratios in both L929 and WEHI 164 cells ($P < 0.05$). The cytotoxicity of synthetic pDNA-PEI-CeO_2 NPs was less than pDNA-PEI 10 kDa in L929 cells (Fig. 8A) at the C/P 2, 4, and 6. In WEHI 164 cells (Fig. 8B), cytotoxicity of synthetic pDNA-PEI-CeO_2 NPs was less than pDNA-PEI 10 kDa at the C/P 2, 4, and 6.

There was significant difference in cytotoxicity effect of pDNA-PEI-CeO_2 NPs between normal cells (L929) and cancer cells (WEHI 164), so

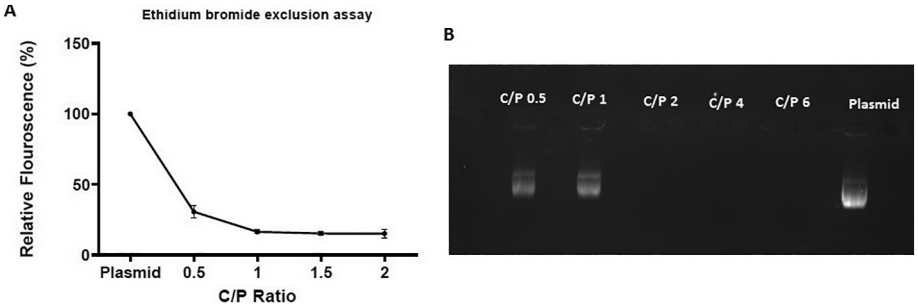

Fig. 6. A) EtBr assay using EGFP plasmid DNA for investigation of the ability of PEI-CeO_2 NPs to condensation of pDNA.
B) Gel retardation assay to evaluate the condensation ability of PEI-CeO_2 NPs with pDNA in C/P ratios from 0.5 to 6.

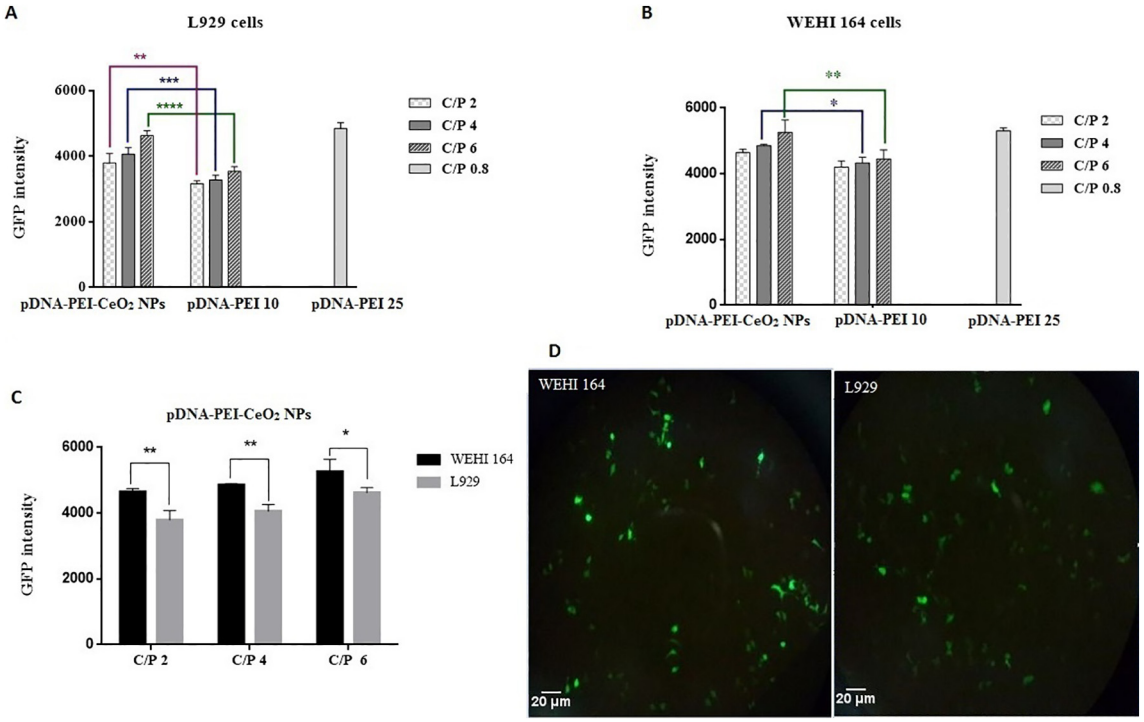

Fig. 7. Transfection efficiency of pDNA-PEI-CeO_2 NPs in A) L929 cells, and B) WEHI 164 cells in C/P ratios of 2, 4 and 6. C) Comparison of transfection efficiency of pDNA-PEI-CeO_2 NPs in L929 cells and WEHI 164 cells. D) Fluorescence microscope images of EGFP expression in WEHI 164 and L929 cells transfected with pDNA-PEI-CeO_2 NPs, magnification 10×.

that pDNA-PEI-CeO_2 NPs had higher cytotoxicity in the WEHI 164 cells than L929 cells at the C/P 2, 4, and 6 (Fig. 8C).

Furthermore, in comparison with pDNA-PEI 25 kDa (C/P 0.8), the prepared pDNA-PEI-CeO_2 NPs at all C/P ratios showed significantly lower cytotoxicity in both L929 and WEHI 164 cells ($P < 0.05$).

3.8. Apoptosis assay

The potential effects of pDNA-PEI-CeO_2 NPs for induction of apoptosis were evaluated by annexin V/PI double staining (Fig. 9) in L929 and WEHI 164 cells.

As shown in Fig. 10A, pDNA-PEI-CeO_2 NPs were able to induce more apoptosis in L929 cells in comparison to pDNA-PEI and pDNA-CeO_2 NPs control groups. Also as shown in Fig. 10B, in WEHI 164 cells,

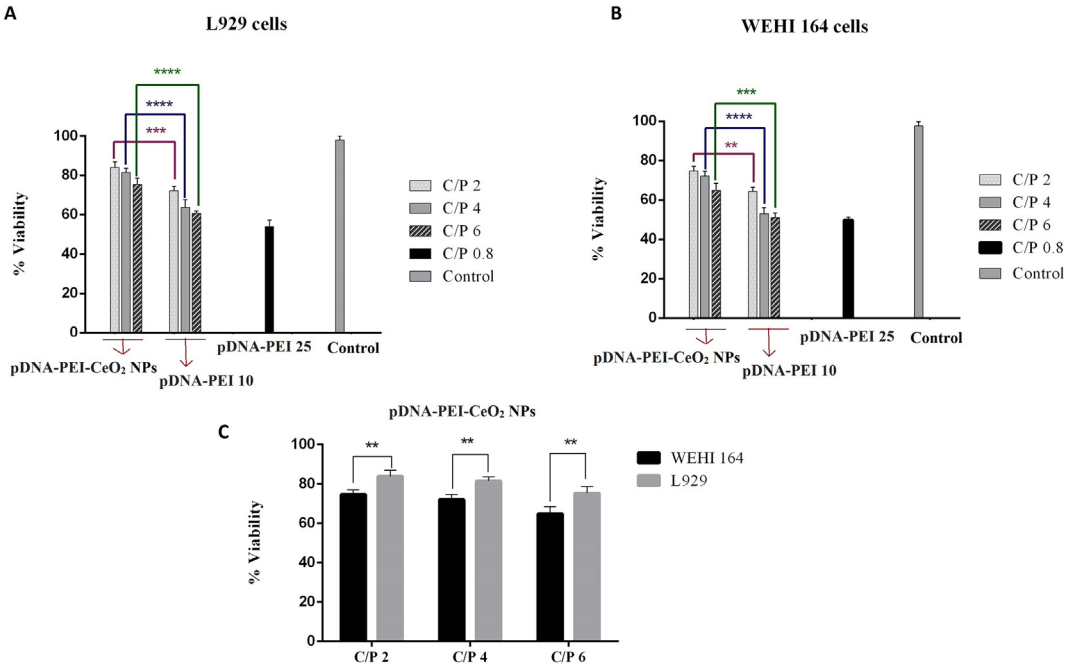

Fig. 8. Cytotoxicity assay of pDNA-PEI-CeO_2 NPs in A) L929 cells, and B) WEHI 164 cells in C/P ratios of 2, 4 and 6. C) Comparison of cytotoxicity of pDNA-PEI-CeO_2 NPs in L929 cells and WEHI 164 cells.

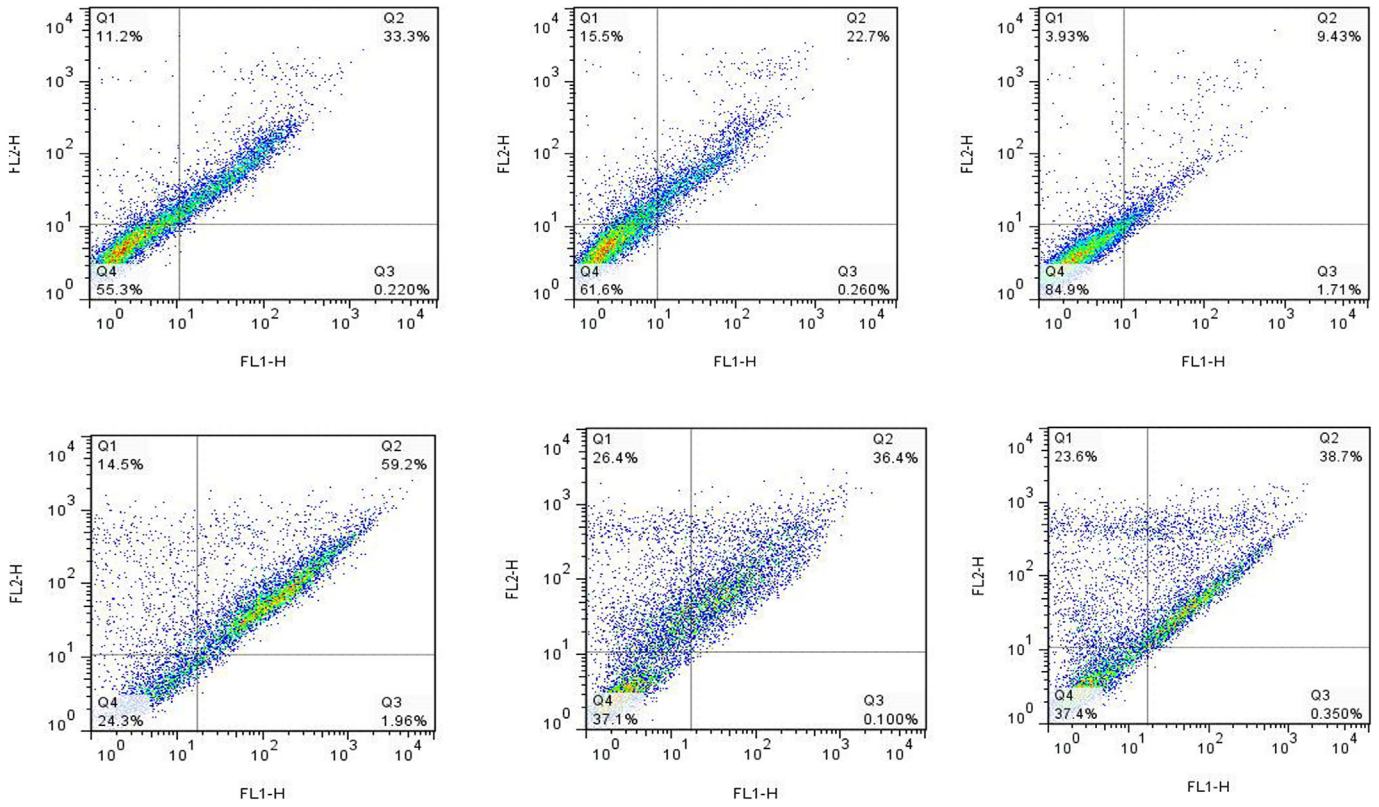

Fig. 9. Representative dot plots of flow cytometry analysis of annexin V/PI staining of A) L929 cells, and B) WEHI 164 cells treated with pDNA-PEI-CeO_2 NPs and control groups.

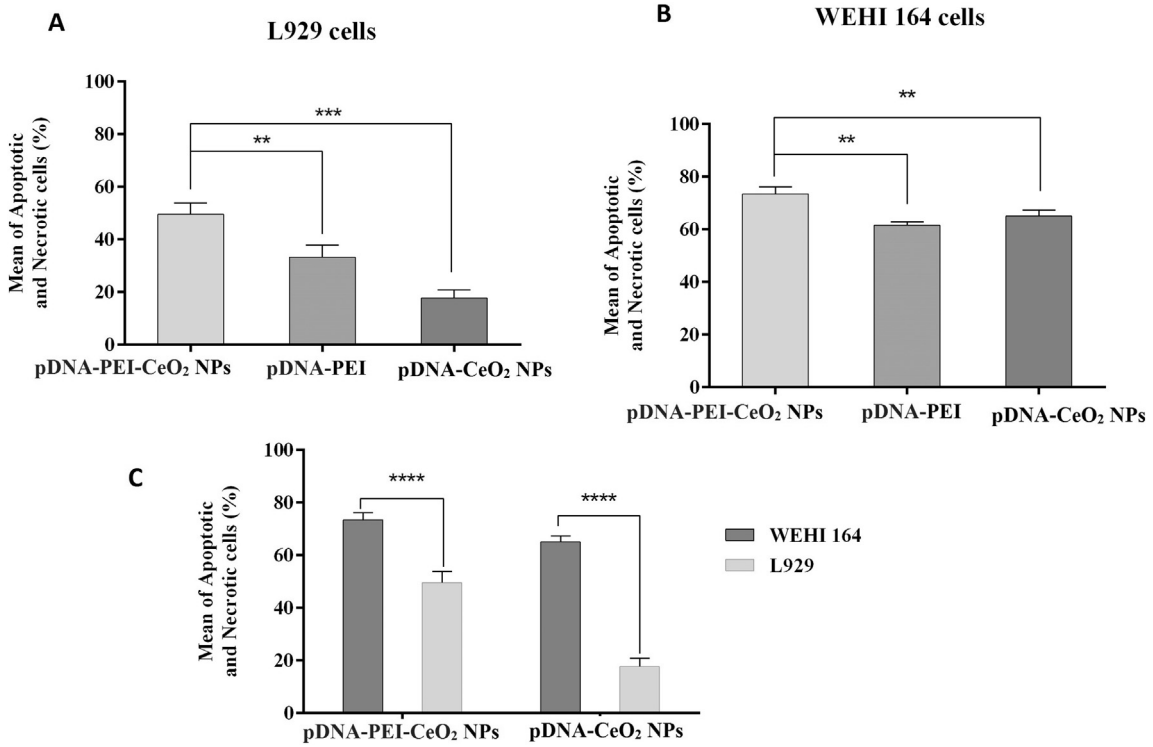

Fig. 10. Apoptosis assay of pDNA-PEI-CeO_2 NPs in A) L929 cells, and B) WEHI 164 cells in C/P 4. C) Comparison between percentage of the apoptotic and necrotic cells in WEHI 164 and L929 cells after treatment with pDNA-PEI-CeO_2 NPs and pDNA-CeO_2 NPs.

pDNA-PEI-CeO_2 NPs induced more apoptosis compared with pDNA-PEI and pDNA-CeO_2 NPs control groups.

There was significant difference in apoptosis effect of pDNA-PEI-CeO_2 NPs between the normal cells (L929) and cancer cells (WEHI 164), so that induction of apoptosis in the cancer cells was more than normal cells (Fig. 10C). Moreover, in CeO_2-NPs control group, pDNA-CeO_2 NPs alone induced more apoptosis in WEHI 164 cells than L929 cells (Fig. 10C).

4. Discussion

In the present study, we examined the properties of PEI-CeO_2 NPs as a non-viral gene delivery vector. We investigated pDNA-PEI-CeO_2 NPs transfection efficiency and cytotoxicity on WEHI 164 cancer cells and normal L929 cells. CeO_2-NPs were prepared through green method as describe previously. PEI was chosen as an ideal candidate due to its good DNA condensation ability. The synthesis of PEI-CeO_2 NPs confirmed by TEM, FE-SEM, EDX, and FTIR methods.

One of the important factors for achieving efficient gene delivery is the ability of nanocarriers to binding and condensing of nucleic acid [40]. It is notable that higher DNA condensation capability is more desirable for gene delivery purposes. PEI-CeO_2 NPs were able to effectively condense DNA molecules via electrostatic interactions at C/P ratio of 0.5 because of positively charged pDNA-PEI-CeO_2 NPs formation (Fig. 6). PEI has a high positively charge density leading to reduction of particle size (~100 nm or less) that are capable to improve transfection efficacy in vitro and in vivo. Also tight interaction between PEI and pDNA protects pDNA from nuclease degradation. PEI polymer is able to confer a remarkably more efficient protection against nuclease degradation than other polycationic polymers [41].

The particle size and surface charge of nanocarriers are major factors that affecting cell transfection and toxicity [42]. As summarized in Table 1, the size and zeta potential of pDNA-PEI-CeO_2 NPs were 124 ± 7 nm and 22 ± 2 mV, respectively. Nanoparticles with positive charge through electrostatic interaction by negatively charged of cell surface are able to enter the cells [43]. Therefore the positive charge of pDNA-PEI-CeO_2 NPs leads to more cellular uptake and more transfection efficacy. Overall, PEI-CeO_2 NPs had proper physicochemical properties for gene delivery.

Recently, oxide nanoparticles such as CeO_2 [44], zinc oxide (ZnO) [45], magnetite (Fe_3O_4) [4,46], silicon dioxide (SiO_2) [5,47], and graphene oxide (GO) [48,49] attract much attention as potential drug and gene delivery carriers due to their versatile physiochemical properties, such as nanoscale size, easy synthesis, tailorable surface charge density, facile surface functionalization, good biocompatibility, and low toxicity [9]. In the present study, the PEI-CeO_2 NPs were able to transfer the pDNA (EGFP reporter gene) into the cells. As demonstrated in Fig. 7, the transfection efficacy of prepared pDNA-PEI-CeO_2 NPs increased with increasing C/P ratios in both L929 and WEHI 164 cells. This is due to increase of PEI content of NPs by increasing the C/P ratios, which not only increases the charge of particles and facilitates entry into cells and nuclei, but also augments endosomal escape of particles [50,51]. Therefore increasing C/P ratios could improve the transfection efficiency.

In this study we showed that the transfection efficacy of prepared pDNA-PEI-CeO_2 NPs improved compared to pDNA-PEI in both L929 (Fig. 7A) and WEHI 164 (Fig. 7B) cells. It was also observed (Fig. 7C) that the transfection efficacy in tumor cells (WEHI 164) was higher than normal cells (L929). It seems that presence of CeO_2-NPs in the pDNA-PEI-CeO_2 NPs helps to improve transfection efficiency of PEI in different ways including enhancement of both cellular and nuclear uptake and reduction of toxicity. Das et al. developed dimethyldioctadecylammonium bromide (DODAB)-CeO_2 hybrids as a new nanovector for gene delivery [44]. CeO_2/DODAB-pDNA nanoparticles had higher cellular uptake and transfection compared to DODAB-pDNA complexes. They confirmed that the coating of DODAB onto the surface of CeO_2 led to the formation of smaller particles and inhibiting the formation of large multilamellar structure that resulting in enhanced cellular uptake and gene delivery. Moreover, they suggested that the higher cytotoxicity of DODAB compared to CeO_2/DODAB vectors may restrict the subsequent transcription of the DNA into mRNA and translation into proteins. Also it seems that the presence of CeO_2-NPs in the pDNA-PEI-CeO_2 NPs could facilitate nuclear transport of pDNA-PEI-CeO_2 NPs. Chen et al. proved ZnO microflowers could be used to enhance the gene expression level of PEI (MW = 1.8 kDa). They suggested that ZnO's help to penetrate into the cell membrane is the possible reason of higher gene transfection of ZnO-PEI/pDNA compared to PEI/pDNA alone [45]. Zarei et al. modified the surface of mesoporous silica nanoparticles (MSNs) with PEI. They suggested that better transfection efficiency of PEI coated MSNs compared to unmodified PEI, can be due to the ability of MSNs to concentrate and settle the pDNA on the cell surface which improves the cellular uptake of pDNA [47].

The cytotoxicity of a carrier considered as an important parameter for successful gene delivery. In the present study (Fig. 8), the MTT assay of pDNA-PEI-CeO_2 NPs indicates an increase in cytotoxicity through the increase of C/P ratios in both L929 and WEHI 164 cells. Calculation of C/P ratio was based on the PEI portion of PEI-CeO_2 NPs (constant amount of pDNA) so by increasing the C/P ratios, the PEI content of pDNA-PEI-CeO_2 NPs that have positive charge were increased which in turn could induce more toxicity. Recent investigations demonstrated that by increasing the C/P ratios, nanoparticles showed more positively charges, which led to more transfection and less cell viability [50,52]. Electrostatic interactions between cationic particles and negatively-charged of cell surface membranes cause cell damage and cytotoxicity [53,54]. Therefore excessive positive charge of nanocarriers leads to increase in cytotoxicity. Furthermore, another reason for cytotoxicity of PEI is the effects on the proton pump activity [55]. In this study we showed that the cytotoxicity of synthetic pDNA-PEI-CeO_2 NPs was less than pDNA-PEI in both L929 and WEHI 164 cells. Similarly, Das et al. indicated that CeO_2/DODAB vectors showed less toxicity and greater biocompatibility than unmodified DODAB [44]. Chen et al. suggested that the lower cytotoxicity of ZnO-PEI/pDNA than PEI/pDNA could be due to the shielding the positive charges of PEI [45]. It seems that presence of CeO_2-NPs in the pDNA-PEI-CeO_2 NPs was led to the covering the excessive positive charge and amine groups of PEI consequently reduced the cytotoxicity of PEI.

Perez et al. showed that CeO_2-NPs have pH-dependent antioxidant properties, which promote cell survival under conditions of oxidative stress and protects normal cells against free radicals but cannot protect cancerous cells, which have normally acidic pH. Therefore CeO_2-NPs have a potential clinical use especially for treatment of cancer [56]. Similarly, in our study pDNA-PEI-CeO_2 NPs showed more toxicity in cancer cells than normal cells (Fig. 8C).

Moreover, the synthesized PEI-CeO_2 NPs (Fig. 2) were well dispersed in distilled water and did not precipitate even after 24 h which is essential for biological applications, so modification of CeO_2-NPs by PEI could improve water solubility of CeO_2-NPs and enhance its therapeutic effects. Das et al. used CeO_2 as drug delivery vehicle for delivery of the anti-cancer drug doxorubicin (DOX) to human ovarian cancer cells. CeO_2/DOX showed higher cellular uptake, drug release behaviors, cell proliferation inhibition, and apoptosis compared to free DOX. CeO_2 has a pH-dependent surface charge therefore DOX was released faster from CeO_2/DOX in reductive acidic conditions (pH 5.0, 10 mM glutathione) than pH 7.4. They mentioned that this pH/reduction dual-sensitive drug carrier would not only decrease the amount of drug loss to the blood circulation but would also undergo drug release during the endocytosis, thus enhancing the therapeutic efficacy [57]. Sack et al. displayed CeO_2-NPs augmented the antitumor activity of DOX in human melanoma cells. In contrast, CeO_2-NPs protected human dermal fibroblasts from DOX-induced cytotoxicity [58].

Our data indicated that the pDNA-PEI-CeO_2 NPs could induce apoptosis in cells. In both WEHI 164 cancer cells and L929 normal cells,

pDNA-PEI-CeO_2 NPs led to the more apoptosis than pDNA-PEI and pDNA-CeO_2 NPs control groups (Fig. 10). Also there was significant difference in apoptosis effect of pDNA-PEI-CeO_2 NPs between the normal cells and cancer cells, so that induction of apoptosis in the cancer cells was more than normal cells (Fig. 10C). This result is consistent with cytotoxicity assay, which showed that pDNA-PEI-CeO_2 NPs exhibited higher toxicity in cancerous cells than normal cells (Fig. 8C).

In both cancer and normal cells, the cytotoxicity of pDNA-PEI-CeO_2 NPs was less than pDNA-PEI, but pDNA-PEI-CeO_2 NPs induced more apoptosis in compare with pDNA-PEI. This difference could be related to the two phase cytotoxicity of PEI [59]. The viability assay (MTT) indicate phase I cytotoxicity of PEI, in which electrostatic interactions between positive charge of PEI and negatively-charged of cell membrane leads to plasma membrane disruption (within 30 min of exposure) [54]. It seems that presence of CeO_2-NPs in the pDNA-PEI-CeO_2 NPs was led to the covering the excessive positive charge and amine groups of PEI consequently reduced the cytotoxicity of PEI. Apoptosis reflects phase II cytotoxicity of PEI, in which PEI induce channel formation in the outer mitochondrial membrane followed by activation of a mitochondrially mediated apoptosis [59]. Hence pDNA-PEI-CeO_2 NPs induced more apoptosis than pDNA-PEI.

Therefore pDNA-PEI-CeO_2 NPs have two different behaviors in cancerous and normal cells and are an appropriate candidate for gene and drug delivery, gene therapy, and in vivo targeted diagnosis.

5. Conclusions

In this project, we investigated the properties of PEI coated CeO_2-NPs as a novel gene delivery vector. The results of transfection study showed that pDNA-PEI-CeO_2 NPs (C/P = 4) are a suitable carrier for gene delivery with low cytotoxicity. pDNA-PEI-CeO_2 NPs displayed more transfection, cytotoxicity, and apoptosis in cancer cells than normal cells. Because of the antioxidative property of CeO_2-NPs towards normal cells, pDNA-PEI-CeO_2 NPs may offer a novel approach in cancer treatment by reduce the side effects on normal cells. Also pDNA-PEI-CeO_2 NPs can be considered as a combination therapy or pDNA-PEI-CeO_2 NPs mediated supplementation therapy with conventional chemotherapeutics for synergistic effects to improve the therapeutic outcome.

Acknowledgments

We would like to acknowledge for the financial support from Mashhad University of Medical Sciences, Mashhad, Iran providing financial support and facilities and equipment for this research (Grant number: 940568) based on the Ph.D. thesis of Ms. L. Hasanzadeh.

Declaration of Competing Interest

There is no conflict of interest in this study.

References

[1] S. Patnaik, K.C. Gupta, Novel polyethylenimine-derived nanoparticles for in vivo gene delivery, Expert Opin. Drug Deliv. 10 (2) (2013) 215–228.
[2] A. Hall, et al., Polyplex evolution: understanding biology, optimizing performance, Mol. Ther. 25 (7) (2017) 1476–1490.
[3] H.H. Yiu, et al., Novel magnetite-silica nanocomposite (Fe_3O_4-SBA-15) particles for DNA binding and gene delivery aided by a magnet array, J. Nanosci. Nanotechnol. 11 (4) (2011) 3586–3591.
[4] Y. Wang, et al., A magnetic nanoparticle-based multiple-gene delivery system for transfection of porcine kidney cells, PLoS One 9 (7) (2014) e102886.
[5] Y.K. Buchman, et al., Silica nanoparticles and polyethyleneimine (PEI)-mediated functionalization: a new method of PEI covalent attachment for siRNA delivery applications, Bioconjug. Chem. 24 (12) (2013) 2076–2087.
[6] K. Kunath, et al., Low-molecular-weight polyethylenimine as a non-viral vector for DNA delivery: comparison of physicochemical properties, transfection efficiency and in vivo distribution with high-molecular-weight polyethylenimine, J. Control. Release 89 (1) (2003) 113–125.
[7] U. Lungwitz, et al., Polyethylenimine-based non-viral gene delivery systems, Eur. J. Pharm. Biopharm. 60 (2) (2005) 247–266.
[8] V. Sokolova, M. Epple, Inorganic nanoparticles as carriers of nucleic acids into cells, Angew. Chem. Int. Ed. 47 (8) (2008) 1382–1395.
[9] Z.P. Xu, et al., Inorganic nanoparticles as carriers for efficient cellular delivery, Chem. Eng. Sci. 61 (3) (2006) 1027–1040.
[10] E. Nourmohammadi, et al., Cytotoxic activity of greener synthesis of cerium oxide nanoparticles using carrageenan towards a WEHI 164 cancer cell line, Ceram. Int. 44 (16) (2018) 19570–19575.
[11] B. Nelson, et al., Antioxidant cerium oxide nanoparticles in biology and medicine, Antioxidants 5 (2) (2016) 15.
[12] A. Asati, et al., Oxidase-like activity of polymer-coated cerium oxide nanoparticles, Angew. Chem. 121 (13) (2009) 2344–2348.
[13] S. Kargozar, et al., Biomedical applications of nanoceria: new roles for an old player, Nanomedicine 13 (23) (2018) 3051–3069.
[14] C. Korsvik, et al., Superoxide dismutase mimetic properties exhibited by vacancy engineered ceria nanoparticles, Chem. Commun. (10) (2007) 1056–1058.
[15] T. Pirmohamed, et al., Nanoceria exhibit redox state-dependent catalase mimetic activity, Chem. Commun. 46 (16) (2010) 2736–2738.
[16] J.M. Dowding, et al., Cellular interaction and toxicity depend on physicochemical properties and surface modification of redox-active nanomaterials, ACS Nano 7 (6) (2013) 4855–4868.
[17] C. Xu, et al., Nucleoside triphosphates as promoters to enhance nanoceria enzyme-like activity and for single-nucleotide polymorphism typing, Adv. Funct. Mater. 24 (11) (2014) 1624–1630.
[18] F. Pagliari, et al., Cerium oxide nanoparticles protect cardiac progenitor cells from oxidative stress, ACS Nano 6 (5) (2012) 3767–3775.
[19] K.L. Heckman, et al., Custom cerium oxide nanoparticles protect against a free radical mediated autoimmune degenerative disease in the brain, ACS Nano 7 (12) (2013) 10582–10596.
[20] M.S. Wason, J. Zhao, Cerium oxide nanoparticles: potential applications for cancer and other diseases, Am. J. Transl. Res. 5 (2) (2013) 126.
[21] A. Shcherbakov, et al., Advances and prospects of using nanocrystalline ceria in cancer theranostics, Russ. J. Inorg. Chem. 59 (13) (2014) 1556–1575.
[22] V. Shah, et al., Antibacterial activity of polymer coated cerium oxide nanoparticles, PLoS One 7 (10) (2012) e47827.
[23] M. Thomas, A.M. Klibanov, Enhancing polyethylenimine's delivery of plasmid DNA into mammalian cells, Proc. Natl. Acad. Sci. 99 (23) (2002) 14640–14645.
[24] A. Pathak, S. Patnaik, K.C. Gupta, Recent trends in non-viral vector-mediated gene delivery, Biotechnol. J. 4 (11) (2009) 1559–1572.
[25] M. Hashemi, et al., Modified polyethyleneimine with histidine–lysine short peptides as gene carrier, Cancer Gene Ther. 18 (1) (2011) 12.
[26] C.-H. Ahn, et al., Biodegradable poly (ethylenimine) for plasmid DNA delivery, J. Control. Release 80 (1–3) (2002) 273–282.
[27] J. Glasel, Validity of nucleic acid purities monitored by 260 nm/280 nm absorbance ratios, Biotechniques 18 (1) (1995) 62–63.
[28] M.R. Green, J. Sambrook, Molecular cloning, A Laboratory Manual 4th, 2012.
[29] L. Hasanzadeh, et al., Green synthesis of labeled CeO_2 nanoparticles with 99mTc and its biodistribution evaluation in mice, Life Sci. 212 (2018) 233–240.
[30] S. Patil, et al., Surface-derivatized nanoceria with human carbonic anhydrase II inhibitors and fluorophores: a potential drug delivery device, J. Phys. Chem. C 111 (24) (2007) 8437–8442.
[31] A. Cimini, et al., Antibody-conjugated PEGylated cerium oxide nanoparticles for specific targeting of Aβ aggregates modulate neuronal survival pathways, Acta Biomater. 8 (6) (2012) 2056–2067.
[32] S. Askarian, et al., Cellular delivery of shRNA using aptamer-conjugated PLL-alkyl-PEI nanoparticles, Colloids Surf. B: Biointerfaces 136 (2015) 355–364.
[33] S.L. Snyder, P.Z. Sobocinski, An improved 2,4,6-trinitrobenzenesulfonic acid method for the determination of amines, Anal. Biochem. 64 (1) (1975) 284–288.
[34] R.K. Oskuee, et al., Investigating the influence of polyplex size on toxicity properties of polyethylenimine mediated gene delivery, Life Sci. 197 (2018) 101–108.
[35] A.H. Nia, et al., Evaluation of chemical modification effects on DNA plasmid transfection efficiency of single-walled carbon nanotube–succinate–polyethylenimine conjugates as non-viral gene carriers, MedChemComm 8 (2) (2017) 364–375.
[36] H. Yu, V. Russ, E. Wagner, Influence of the molecular weight of bioreducible oligoethylenimine conjugates on the polyplex transfection properties, AAPS J. 11 (3) (2009) 445.
[37] E. Nourmohammadi, et al., Evaluation of anticancer effects of cerium oxide nanoparticles on mouse fibrosarcoma cell line, J. Cell. Physiol. 234 (4) (2019) 4987–4996.
[38] A. Prieto, et al., Apoptotic rate: a new indicator for the quantification of the incidence of apoptosis in cell cultures, Cytometry 48 (4) (2002) 185–193.
[39] I. Vermes, et al., A novel assay for apoptosis flow cytometric detection of phosphatidylserine expression on early apoptotic cells using fluorescein labelled annexin V, J. Immunol. Methods 184 (1) (1995) 39–51.
[40] D.D. Dunlap, et al., Nanoscopic structure of DNA condensed for gene delivery, Nucleic Acids Res. 25 (15) (1997) 3095–3101.
[41] T. Merdan, J. Kopeček, T. Kissel, Prospects for cationic polymers in gene and oligonucleotide therapy against cancer, Adv. Drug Deliv. Rev. 54 (5) (2002) 715–758.
[42] R. Kazemi Oskuee, et al., Preparation, characterization and transfection efficiency of nanoparticles composed of alkane-modified polyallylamine, Nanomed. J. 2 (2) (2015) 111–120.
[43] A. Dehshahri, et al., Gene transfer efficiency of high primary amine content, hydrophobic, alkyl-oligoamine derivatives of polyethylenimine, Biomaterials 30 (25) (2009) 4187–4194.
[44] J. Das, et al., Cationic lipid-nanoceria hybrids, a novel nonviral vector-mediated

gene delivery into mammalian cells: investigation of the cellular uptake mechanism, Sci. Rep. 6 (2016) 29197.
[45] M. Chen, et al., Enhanced gene delivery of low molecular weight PEI by flower-like ZnO microparticles, Mater. Sci. Eng. C 69 (2016) 1367–1372.
[46] A.F. Jorge, et al., Combining polyethylenimine and Fe (III) for mediating pDNA transfection, Biochim. Biophys. Acta, Gen. Subj. 1850 (6) (2015) 1325–1335.
[47] H. Zarei, et al., Enhanced gene delivery by polyethyleneimine coated mesoporous silica nanoparticles, Pharm. Dev. Technol. 24 (1) (2019) 127–132.
[48] L. Zhang, et al., Enhanced chemotherapy efficacy by sequential delivery of siRNA and anticancer drugs using PEI-grafted graphene oxide, Small 7 (4) (2011) 460–464.
[49] H. Kim, et al., Graphene oxide–polyethylenimine nanoconstruct as a gene delivery vector and bioimaging tool, Bioconjug. Chem. 22 (12) (2011) 2558–2567.
[50] R. Cheraghi, et al., Optimization of conditions for gene delivery system based on PEI, Nanomed. J. 4 (1) (2017) 8–16.
[51] Q. Xie, et al., PEI/DNA formation affects transient gene expression in suspension Chinese hamster ovary cells via a one-step transfection process, Cytotechnology 65 (2) (2013) 263–271.
[52] Z.R. Amin, et al., The effect of cationic charge density change on transfection efficiency of polyethylenimine, Iran. J. Basic Med. Sci. 16 (2) (2013) 150.
[53] J. Kloeckner, et al., Gene carriers based on hexanediol diacrylate linked oligoethylenimine: effect of chemical structure of polymer on biological properties, Bioconjug. Chem. 17 (5) (2006) 1339–1345.
[54] A.C. Hunter, Molecular hurdles in polyfectin design and mechanistic background to polycation induced cytotoxicity, Adv. Drug Deliv. Rev. 58 (14) (2006) 1523–1531.
[55] T. Xia, et al., Cationic polystyrene nanosphere toxicity depends on cell-specific endocytic and mitochondrial injury pathways, ACS Nano 2 (1) (2007) 85–96.
[56] J.M. Perez, et al., Synthesis of biocompatible dextran-coated nanoceria with pH-dependent antioxidant properties, Small 4 (5) (2008) 552–556.
[57] J. Das, et al., Nanoceria-mediated delivery of doxorubicin enhances the anti-tumour efficiency in ovarian cancer cells via apoptosis, Sci. Rep. 7 (1) (2017) 9513.
[58] M. Sack, et al., Combination of conventional chemotherapeutics with redox-active cerium oxide nanoparticles-a novel aspect in cancer therapy, Mol. Cancer Ther. 13 (7) (2014) 1740–1749.
[59] S.M. Moghimi, et al., A two-stage poly (ethylenimine)-mediated cytotoxicity: implications for gene transfer/therapy, Mol. Ther. 11 (6) (2005) 990–995.